IEEE Photonics Journal
An IEEE Photonics Society Publication

A Microwave Frequency Measurement System Based on Si3N4 Ring-Assisted Mach-Zehnder Interferometer

Volume 12, Number 4, August 2020

Hao Zhang
Pengfei Zheng
Huimin Yang
Guohua Hu
Binfeng Yun
Yiping Cui

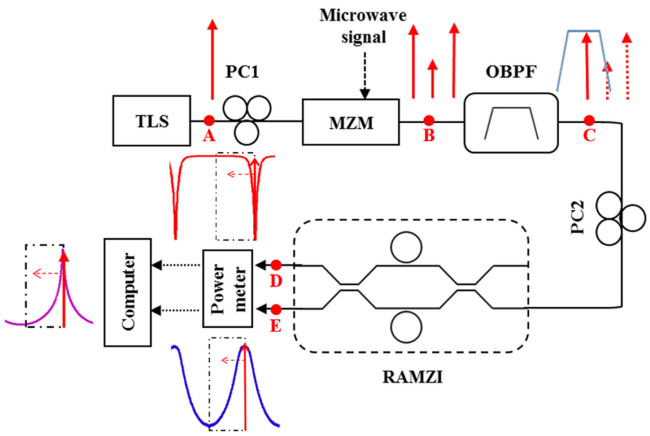

DOI: 10.1109/JPHOT.2020.3004166

IEEE photonics SOCIETY
IEEE

A Microwave Frequency Measurement System Based on Si3N4 Ring-Assisted Mach-Zehnder Interferometer

Hao Zhang, Pengfei Zheng, Huimin Yang, Guohua Hu, Binfeng Yun, and Yiping Cui

Advanced Photonics Center, Southeast University, Nanjing 210096, China

DOI:10.1109/JPHOT.2020.3004166

Manuscript received April 21, 2020; revised June 16, 2020; accepted June 18, 2020. Date of publication June 22, 2020; date of current version July 14, 2020. This work was supported by the National Key R&D Program of China under Grant (2018YFB2201800) and Postgraduate Research & Practice Innovation Program of Jiangsu Province under Grant (KYCX19_0066). Corresponding author: Binfeng Yun (e-mail: ybf@seu.edu.cn.)

Abstract: A microwave frequency measurement system based on a ring assisted Mach-Zehnder interferometer (RAMZI) with a large measurement range and high accuracy is proposed and experimentally demonstrated. By using single-sideband modulation, the microwave signal with unknown frequency is converted to an optical sideband signal, which is used to probe the two complementary output optical powers of the ring-assisted Mach-Zehnder interferometer, then a fixed frequency-to-power mapping is established by obtaining a highly linear amplitude comparison function (ACF). High-precision frequency measurement with a root mean square error (RMSE) of less than 30 MHz was achieved in a frequency range of 5.2 GHz, and relative low-precision frequency measurement with a RMSE of less than 102 MHz was achieved in a frequency range of 11 GHz. Besides, in order to break the trade-off between measurement range and measurement accuracy, a multi-band measurement method was implemented and frequency measurement range of 5∼39 GHz with RMSE lower than 37 MHz was achieved.

Index Terms: Microwave frequency measurement, microwave photonics, ring assisted Mach-Zehnder interferometer.

1. Introduction

Frequency measurement technology has played an irreplaceable role in modern electronic warfare (EW) applications, especially in radar systems. It has been difficult for the traditional electronic system to meet the further development of frequency measurement requirements because its measurement range is limited by the bandwidth of electronic components [1]. In recent years, microwave technology and optics have merged to form microwave photonics (MWP) [2]. With the advantages of both optical and microwave technologies, this new discipline shows excellent performance in the field of frequency measurements, such as wider measurement range, low-loss, lightweight, and immunity to electromagnetic interference (EMI) [3]. Recently, numerous approaches based on MWP have been proposed [4]. In general, there are roughly three different types of microwave photonic frequency measurement schemes, which are based on time-domain scanning [5]–[12], photonic-assisted channelization [13]–[18] systems and frequency-to-power mapping [19]–[38].

In a time-domain scanning systems, by scanning the laser wavelength [5]–[9] or the filter wavelength [10]–[12], the optical carrier and the first-order sideband containing the frequency information will align the filter frequency successively. Therefore, the frequency of the microwave signal can be judged by the time interval between the occurrence of the two filtered optical signals. In this method, the measurement range is closely related to the scan time. If the measurement range is enlarged, the measurement time will also increase, which is not conducive to instantaneous measurement in a wide frequency range. Besides, the measurement resolution will be determined by the filter's bandwidth.

In the systems based on photonic-assisted channelization [13]–[18], the first-order sideband containing the frequency information falls into one optical channel at a specific frequency band. The output power of each channel is monitored. Once an optical signal is detected at the output of a channel, the frequency of the microwave signal can be inferred from the frequency band of the channel. The measurement accuracy of such systems is limited by the channel bandwidth, and the error is usually above 1 GHz.

The main idea of the frequency-to-power mapping systems is to map the frequency of the microwave signal to microwave power [19]–[26] or optical power [27]–[38]. Once a unique relationship between the frequency and the power is established, the frequency value can be indirectly obtained by measuring the power value. The microwave power detection scheme usually based on microwave power attenuation effect [19]–[22] caused by fiber dispersion or microwave filter response [23]–[26]. These systems inevitably require high-speed photodetectors (PDs), which makes the system cost high. However, for optical power mapping system, only low-cost low-speed PDs are needed, which can reduce the system cost effectively. Such schemes are usually implemented by optical mixing [27]–[31] or optical filtering [32]–[38]. In the optical mixing scheme, the system is complex and bulky, and the measurement error is usually large. However, optical filtering scheme does not require a complex mixing system, and shows a better measurement accuracy. In approaches based on optical filtering [32]–[35], complex optical comb filtering modules were used as the core of the system. In order to achieve two different filtering responses, Ref. [32] and Ref. [33] use two laser sources, which make the system large and expensive. Systems in Ref. [34] and Ref. [35] are simplified by using polarizing beam splitter (PBS), but they are sensitive to signal's polarization. Fortunately, these problems can be solved by using an integrated photonic filter chip with complementary transmission responses. Both Ref. [36] and Ref. [37] use the integrated Mach-Zehnder interferometer (MZI) as the optical filter chip and the carrier-suppressed double-sideband (CS-DSB) modulation was used in frequency measurements. The former approach has a measurement range of 5∼15 GHz and a RMSE lower than 200 MHz. And the latter has a measurement range of 4∼18 GHz and a maximum error of 1.9 GHz. In Ref. [38], an add-drop optical ring resonator (ORR) was used as the filter chip, which can achieve measurements with a RMSE of 63 MHz in frequency range of 0.1∼5 GHz or measurements with a RMSE of about 240 MHz in range of 0.5∼35 GHz. However, high-precision measurement and large bandwidth measurement were implemented with two different chips. Besides, the common limitation of only fixed measurement range were obtained in the approaches proposed in [36]–[38].

In this paper, we propose and experimentally demonstrate a novel approach to achieve microwave frequency measurement with high accuracy and low cost. Comparing with the bulk solutions mentioned in the introduction, the system weight and size can be greatly reduced. The reasons for choosing Si_3N_4 waveguide platform to achieve frequency measurement are as follows: First, comparing with Silicon-On-Insulator (SOI) waveguide, the Si_3N_4 waveguide has much lower propagation loss (∼0.2 dB/cm here), which is critical for obtain high quality ring resonator to achieve high precision frequency measurements. Second, the fabrication process is simpler comparing with SOI waveguide because lithography process with much lower resolution is enough. Third, the Si_3N_4 waveguide has no two-photon absorption effect, which will limit the optical power in the waveguide and degrade the signal noise ration (SNR) of the frequency measurement system. The key device in this system is a low-loss tunable silicon nitride integrated RAMZI [39]. It has two output ports whose transmission spectra are complementary. After calculating the optical power ratio of the two output ports, a high slope ACF can be obtained and frequency measurement

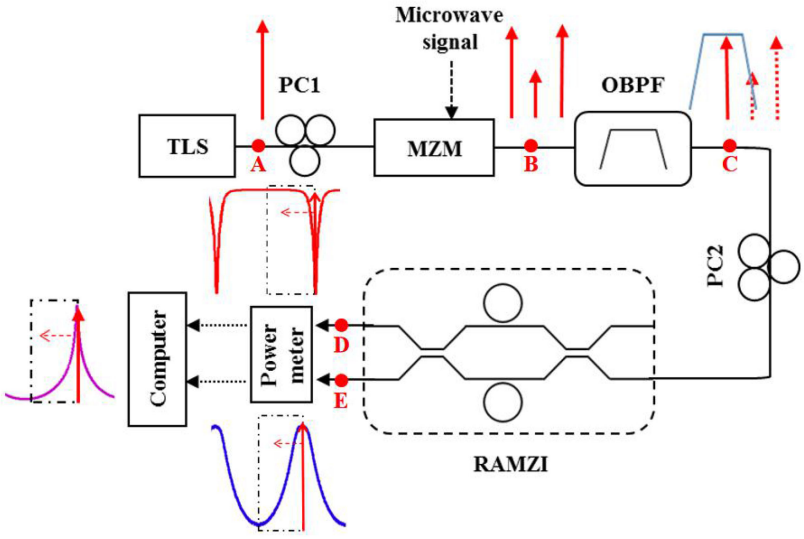

Fig. 1. Schematic diagram of the proposed microwave frequency measurement system. (TLS: tunable laser source, PC: polarization controller, MZM: Mach-Zehnder Modulator, OBPF: optical band-pass filter.)

with high precision was achieved. By tuning the RAMZI, we achieved a high-precision frequency measurement with a RMSE of less than 38 MHz in the frequency range of 5.2 GHz and a relative low-precision frequency measurement with an RMSE of less than 102 MHz in the frequency range of 11 GHz. Besides, by adopting a multi-band measurement approach, the measurement range can be extended to 39 GHz, while the RMSE can still be maintained within 38 MHz, so that the trade-off between measurement range and measurement accuracy is resolved. Comparing with the frequency measurement technologies using the integrated Mach-Zehnder interferometer (MZI) and add-drop optical ring resonator (ORR), the main disadvantage of the proposed RAMZI is more tunable elements are adopted, which will induce more power consumption.

2. Principle

The scheme of the proposed frequency measurement system based on a RAMZI is shown in Fig. 1. A continuous wave (CW) laser carrier is sent into a Mach-Zehnder modulator (MZM), where an unknown microwave signal is modulated on the optical carrier. The MZM is biased at the minimum transmission point (MITP) to produce a CS-DSB signal, which is shown as the spectrum at point B. Subsequently, an tunable optical band-pass filter (OBPF) is used to select the lower sideband (LSB) signal, while rejecting the upper sideband (USB) signal and the residual optical carrier, as shown at point C in Fig. 1. Then a carrier-suppressed single-sideband (CS-SSB) modulation is achieved. As a result, only the LSB signal working as a tunable laser can be launched into the RAMZI, which can be regarded as a pair of filters with complementary filtering response. The filtering responses are shown at points D and E, where the two filtered optical outputs are completely opposite. Then the two filtered optical outputs are detected by a dual-channel optical power meter and sent to a computer for processing. Finally, the ACF, which defined as the detected optical power ratio, is given:

$$ACF\,(f) = \frac{P_1\,(f)}{P_2\,(f)} \tag{1}$$

where f is the microwave frequency to be measured, $P_1(f)$ and $P_2(f)$ are the two output optical powers after the RAMZI. Once the unique relationship between the microwave frequency and ACF

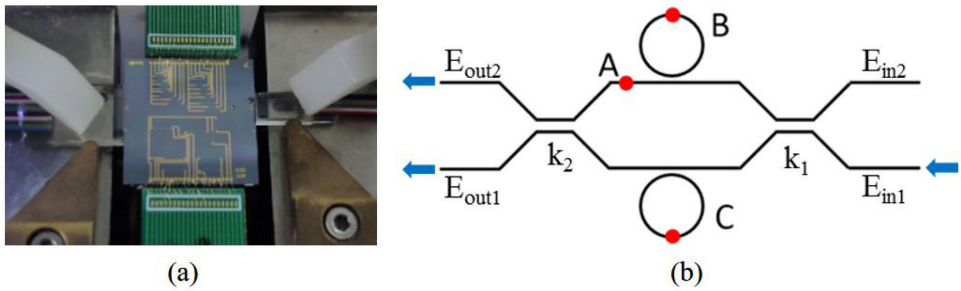

Fig. 2. The (a) picture and (b) structure of the tunable RAMZI chip.

is obtained and calibrated, the microwave frequency can be determined by the measured ACF value.

The picture of the whole chip and structure of the RAMZI chip are shown in Fig. 2. The chip size is 16 mm $\times$ 16 mm, and the RAMZI structure only occupies about 4 mm $\times$ 6 mm. It was fabricated based on the silicon nitride waveguide by using the TriPleX technology [40]. In the RAMZI, two tunable micro-ring resonators (MRRs) with the same perimeter of 2.927 mm are coupled to the two arms of a Mach-Zehnder interferometer (MZI). The corresponding free spectral range (FSR) of the MRR is 60 GHz. By using thermo-optic heaters on the RAMZI chip, three tunable phase shifters are realized, whose locations are represented by red dots A, B, and C in Fig. 2(b). Here due to the unavoidable fabrication error (the resolution is only about 1 μm for the Lionix' MPW service), the initial state of the chip is usually deviated from the design and not optimized for frequency measurements. By adjusting the rings and the MZI with the tunable phase shifters, the fabrication tolerances can be compensated and different optimized ACFs can be obtained for different application scenarios as below.

By using the well known transfer matrix method, the tunable RAMZI can be modeled as:

$$\begin{bmatrix} E_{\text{out2}} \\ E_{\text{out1}} \end{bmatrix} = \begin{bmatrix} \sqrt{1-k_2} & -j\sqrt{k_2} \\ -j\sqrt{k_2} & \sqrt{1-k_2} \end{bmatrix} \begin{bmatrix} e^{-j\varphi}H_1 & 0 \\ 0 & H_2 \end{bmatrix} \begin{bmatrix} \sqrt{1-k_1} & -j\sqrt{k_1} \\ -j\sqrt{k_1} & \sqrt{1-k_1} \end{bmatrix} \begin{bmatrix} E_{\text{in2}} \\ E_{\text{in1}} \end{bmatrix} \tag{2}$$

where E_{in1}, E_{in2} and E_{out1}, E_{out2} are the input and output optical fields, respectively. k_1 and k_2 are the power coupling coefficients of two directional couplers, respectively. φ is the additional phase generated by the variable phase shifter A. The transfer functions of the two MRRs, can be written as follows:

$$H_n = \frac{t - \alpha e^{j(\theta+\psi)}}{1 - \alpha t e^{j(\theta+\psi)}} \ (n = 1 \ or \ 2) \tag{3}$$

Here, t is the self-coupling coefficient of the MRR, α is the transmission factor, θ is the induced round-trip phase shift of the MRR, and ψ is the additional phase shifts generated by variable phase shifter B and C.

When assumed $\alpha = 0.9961$, $t = 0.6739$, $k_1 = 0.7289$ and $k_2 = 0.7783$, the two outputspectra and the their corresponding ACF were simulated and shown in Fig. 3. The curves corresponding to output 1 and output 2 are the spectra at points D and E in Fig. 1, respectively. In our system, the LSB signal containing the microwave frequency information is launched into the RAMZI from one port, as shown by the solid green arrow in Fig. 3. And the wavelength range shown in the black dotted rectangle was selected by the OBPF and regarded as the frequency measurement range. After passing the RAMZI chip, the microwave frequency to be measured can be mapped into the monotonic ACF, which has been calibrated previously. Then the unknown microwave frequency can be measured according to the unique relationship between the microwave frequency and the ACF value.

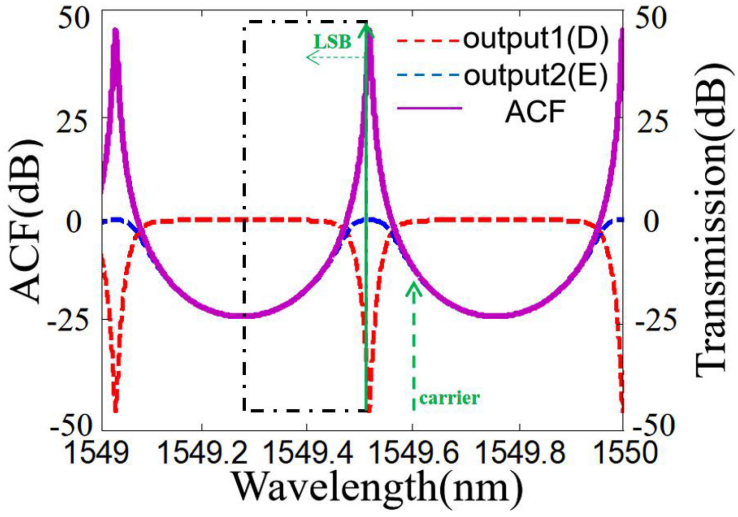

Fig. 3. Schematic diagram of ACF simulation results and measurement principles.

3. Experiment Results

The experiment was conducted in a clean room, and the ambient temperature during the experiments was set as 25 °C. No closed loop temperature control of the chip was used. Before the frequency measurement, we check the spectra of the chip applied with suitable voltages every ten minutes and no obvious spectra variations were observed. However, closed loop temperature control with thermal electric cooler (TEC) should be added if the proposed chip will be used outside.

3.1 High Precision Frequency Measurement in Narrow Frequency Range

As shown in Fig. 1, an optical carrier with 15 dBm power emitted by a tunable laser source (TLS, SANTEC WSL-100) was launched into a 40 GHz MZM (iXblue-1550 MXAN-LN-40) with 3.5 dB insertion loss. By feeding a microwave signal with 15 dBm power from a microwave signal source (Keysight E8257D) into the MZM which was biased at the MITP, a CS-DSB signal was generated. The CS-DSB signal was then introduced into a tunable OBPF (SANTEC OTF-980) to filter out the LSB signal, then a CS-SSB signal can be obtained. For example, Fig. 4 shows the generation process of the CS-SSB signals at 3 GHz. As shown, the optical carrier and the USB signal were suppressed at least 11.8 dB and 31.0 dB, respectively. In the experiment, the bandwidth of tunable OBPF is only 0.05 nm (6.25 GHz) with ultra-high filter slope of 1000 dB/nm (8 dB/GHz). It is true the limited bandwidth of the filter can not achieve very pure CS-SSB signal when the modulation frequency is lower than 3 GHz. Therefore, in the experiments, the measured lowest frequency was chosen as 5 GHz to get at least 30 dB suppression of the optical carrier and one sideband, thus a pure CS-SSB signal were guaranteed. Then, the CS-SSB signal working as a tunable laser was launched into the RAMZI chip. By detecting the two output optical power of the RAMZI chip using a dual-channel optical power meter (THORLABS PM320E), a calibrated ACF which mapped to the microwave frequency can be obtained.

During the chip measurements, it was found when the resonance wavelengths of the two rings were adjusted enough close to each other, the outputs of the RAMZI shown in Fig. 5 basically consistent with the simulation results in Fig. 3. However, the extinction ratio of output2 is very limited, which will degrade the slope of the ACF according to Eq.(1) and limit the frequency measurement precision. In order to get an optimized ACF for high precision frequency measurement, by slightly separating the two rings' resonance wavelengths, a set of output spectra with large extinction ratios

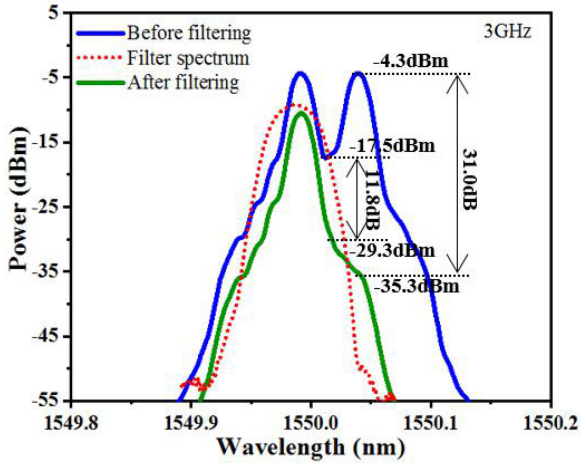

Fig. 4. Optical spectra of the CS-DSB modulation (blue), tunable OBPF (red), and CS-SSB modulation (green).

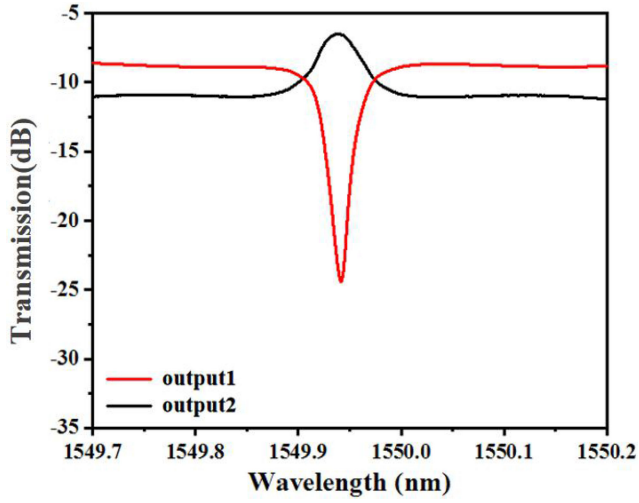

Fig. 5. The measured spectra close to the simulation results.

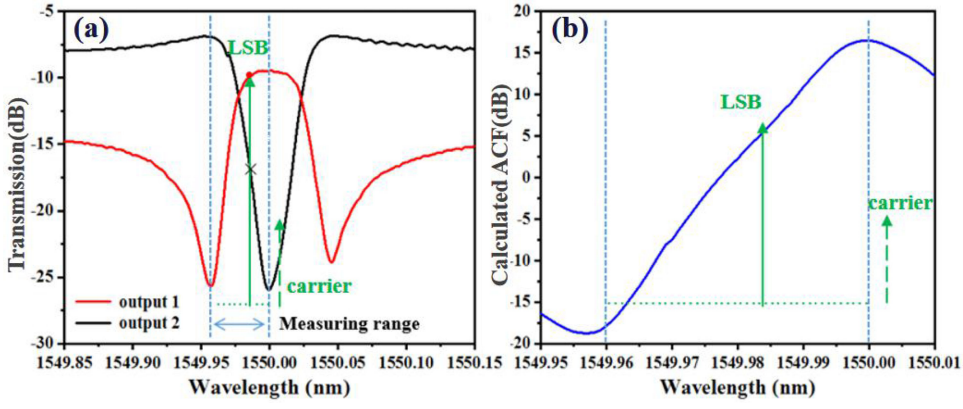

Fig. 6. The (a) transmission spectra and (b) ACF of the RAMZI.

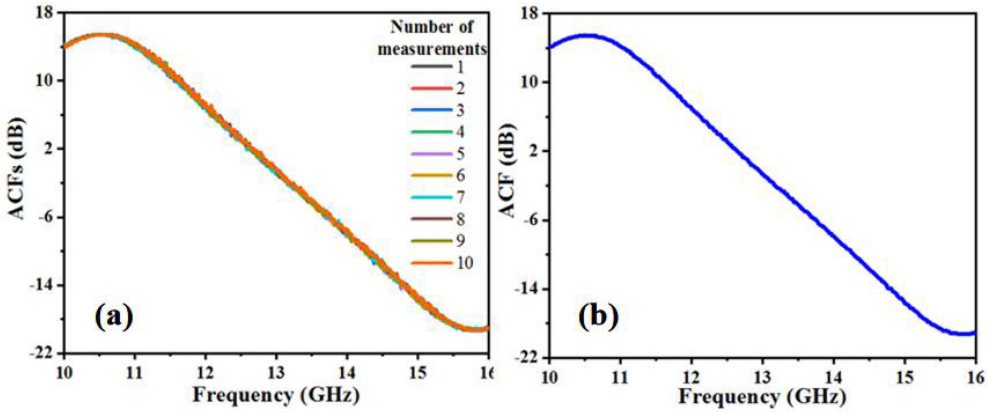

Fig. 7. The (a) ten measurements of the ACF; (b) averaged ACF.

were obtained as shown in Fig. 6(a). Therefore, these output spectra were chosen for high precision microwave frequency measurement.

When the spectra shown in Fig. 6(a) appears, the voltages applied to the phase shifters B and C are 6.9V and 5.35V, respectively. Here the laser carrier wavelength was set as 1550.084 nm, and the wavelength range of 1549.96 nm∼ 1550.00 nm shown between the two blue dotted lines was chosen for frequency measurement. And the corresponding frequency measurement range is 10.5∼15.5 GHz. The ACF in this wavelength range was calculated according to the measured optical transmission spectra and shown in Fig. 6(b). As can be seen, a linear and monotonic ACF in frequency range about 5 GHz was obtained, and a relative large slope of 6.87 dB/GHz was achieved, which is important for high precision frequency measurements.

Then 10 GHz∼16 GHz microwave signal with 20 MHz frequency step from the RF source was input into the frequency measurement system to calibrate the ACF. Ten independent experiments with time span of 1∼2 minutes between each measurement were performed, and the obtained results are shown in Fig. 7(a). It is obvious that good consistency among these measurements were obtained, which indicates the stability of the system. In addition, in the following frequency measurements, the output spectra of the RAMZI chip and corresponding ACF curves were always kept stable in the lab environments. And the averaged ACF shown in Fig. 7(b) was chosen in the following frequency measurements. The slope of the averaged ACF is about 6.73 dB/GHz, which is very close to the calculated result shown in Fig. 6(b).

Here the monotonic and linear part in the middle of the averaged ACF was used for microwave frequency measurements. As can be seen in Fig. 8, microwave signals in the frequency range of 10.5 GHz to 15.7 GHz can be measured, which is very close to the theoretical measurement range shown in Fig. 6(b). In order to verify the measurement errors, the relationship between the measured microwave frequency and the input microwave frequency are shown in Fig. 8(a). And Fig. 8(b) shows the corresponding measurement errors, which are mainly distributed in the frequency range of -60 MHz∼60 MHz, except for few relative large errors about ±180 MHz at lowest frequencies due to the increased nonlinearity of the ACF. It is well known that the maximum errors [37] and RMSE [36] are usually used to evaluate the stability of the system. The maximum error of these ten measurements is limited in −180 MHz∼120 MHz, and the maximum RMSE is less than 30 MHz.

3.2 Low Precision Frequency Measurement in Large Frequency Range

According to the previous theoretical analysis and experiments, it can be seen that the transmission spectrum of the RAMZI chip shown in Fig. 6(a) can only measure microwaves in the frequency range of about 5 GHz. By increasing the voltage applied to the phase shifter C to

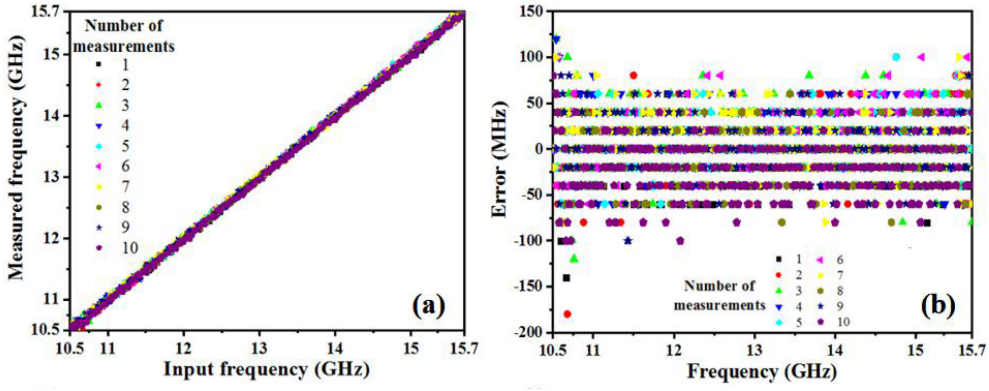

Fig. 8. The relationship between input frequencies and (a) the measured frequencies; (b) the measurement errors.

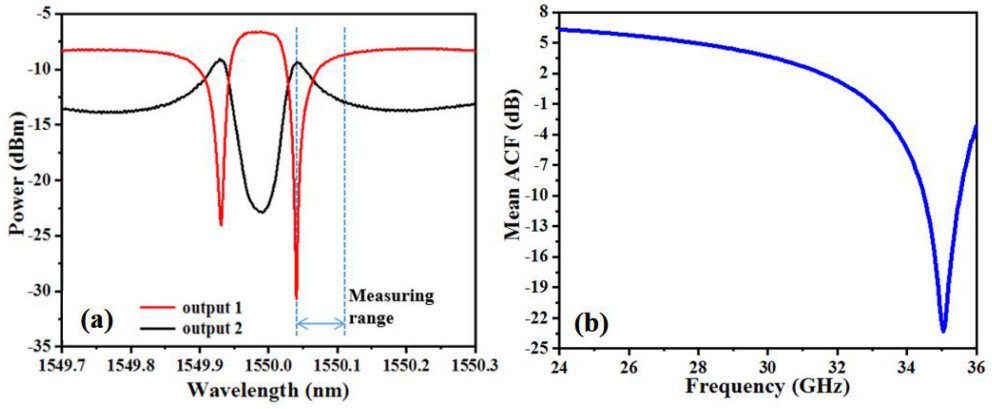

Fig. 9. (a): Transmission spectrum of RAMZI and (b): Mean ACF of ten measurements.

10.1 V, the wavelength difference between the resonances of the two MRRs can be increased and the transmission spectrum of the RAMZI chip shown in Fig. 9(a) was obtained. Under this circumstance, the wavelength range (1550.04 nm∼1550.128 nm) marked by the blue dotted line was selected for frequency measurement. Thanks to the larger monotonic wavelength range, it is possible to achieve frequency measurement with wider frequency range. By setting the laser wavelength as 1553.32 nm and scanning the microwave frequency from 23.5 GHz to 36 GHz with 50 MHz frequency step, an averaged ACF shown in Fig. 9(b) was obtained after ten independent measurements.

In this case, the relationship between the measured and input frequencies in the range of 24-35 GHz is shown in Fig. 10(a), and the measurement error is shown in Fig. 10(b). The maximum measurement error from these ten measurements is limited in ±350 MHz and the maximum value of RMSE is less than 102 MHz. Obviously, compared with the previous scheme, the measurement range is enlarged from 5 GHz to approximately 11 GHz, but the largest RMSE is also increased from 30 MHz to 102 GHz. Therefore, there is a trade-off between measurement range and measurement accuracy.

3.3 Multi-Band Frequency Measurement

In order to achieve frequency measurement with wide range and high accuracy simultaneously, a multi-band frequency measurement scheme as shown in Fig. 11 was proposed. First, the OBPF was used to select the 5 GHz spectral range of the RAMZI with high frequency resolution as

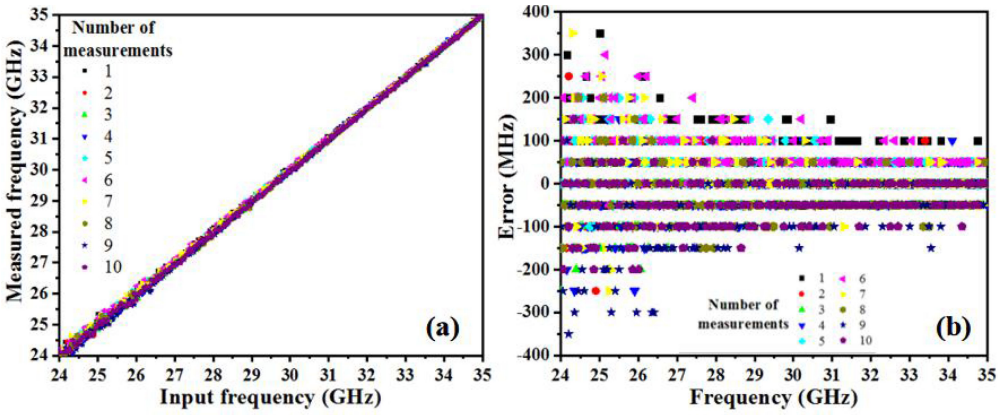

Fig. 10. (a): The relationship between the measured frequency and the input frequency; (b): the measurement errors.

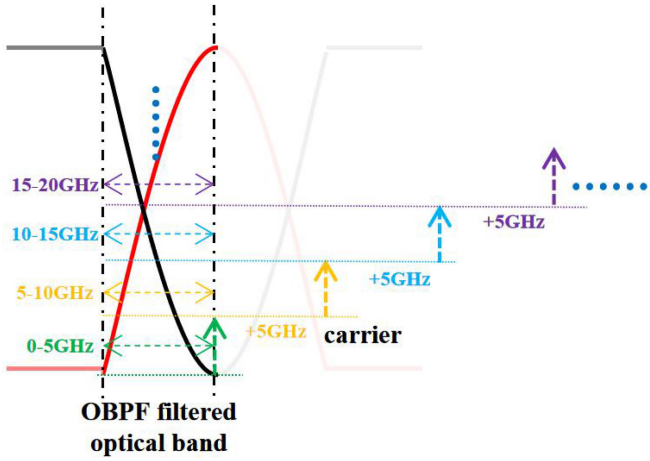

Fig. 11. Schematic diagram of multi-band measurement.

TABLE 1
The Optical Carrier's Wavelengths and the Corresponding Frequency Band to be Measured

Wavelength(nm)	1550.036	1550.072	1550.108	1550.140	1550.172
Frequency Band(GHz)	5-9.2	9-13.6	13.5-18	17.4-21.7	21.5-25.6
Wavelength(nm)	1550.204	1550.236	1550.264	1550.290	
Frequency Band(GHz)	25.5-29.5	29.4-33.2	32.9-36.5	36-39.9	

shown in Fig. 11, so that only optical signals located in this wavelength range can enter the RAMZI chip. Then, by setting different optical carrier's wavelengths with 5 GHz frequency step, the corresponding LSBs located in different frequency bands fall into the selected RAMZI's filtering spectral range, and microwave signals in different frequency bands with 5 GHz bandwidth can be measured each time. Finally, a wider microwave frequency measurement range can be obtained by stitching these narrow frequency bands.

In order to achieve high frequency resolution, the RAMZI transmission spectrum shown in Fig. 6(a) was chosen. In a proof of concept experiment, the optical carrier's wavelengths and their corresponding frequency band to be measured is shown in Table 1.

Since it is difficult for the OBPF to completely remove the out of band signal and the remained very weak residual signal can have a huge impact on measurement results. For example, if two

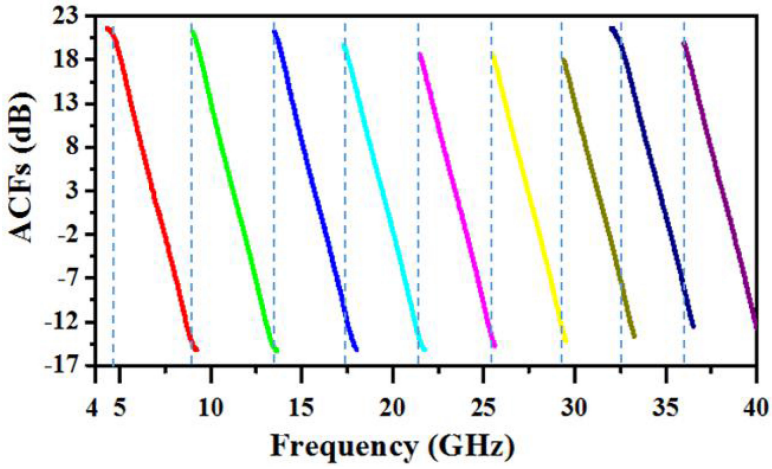

Fig. 12. ACFs for multi-band measurements.

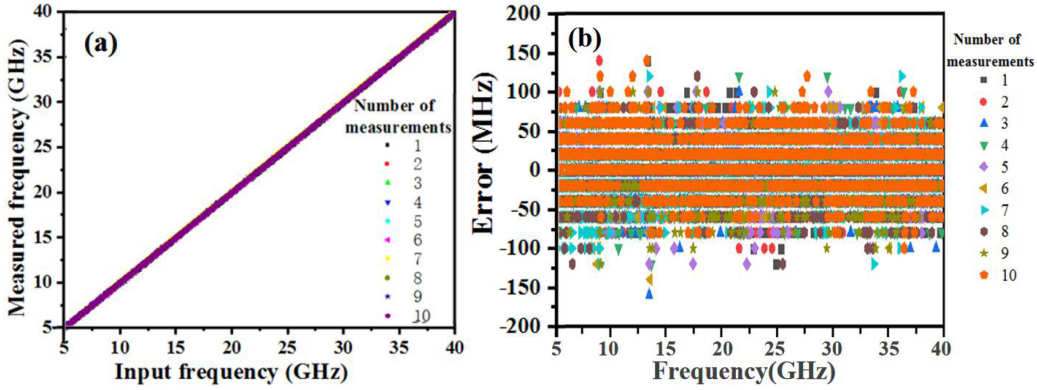

Fig. 13. (a) Relationship between the measured and input frequencies in multi-band measurements; (b) measurement errors.

output power detected by the optical power meters is −70 dBm and −75 dBm, the power ratio will be 5 dB and the wrong microwave frequency will be calculated. A criterion on the two monitored optical powers was introduced to eliminate the obstacles: if the output power of any port is too small (the critical value was selected as −45 dBm in the experiment), it will be regard as noise and ignored. Under this condition, the wavelength of the optical carrier was set according to Table 1 and the RF source was scanned in 20 MHz frequency step in each frequency band to calibrate the ACFs. The multi-band mean ACFs after ten measurements were obtained as shown in Fig. 12.

As the microwave frequency increases, the modulation efficiency will decrease and the output power decreases accordingly. Therefore, when measuring high-frequency microwave signal, it is necessary to reduce the range of ACF to ensure a high-precision measurement result. It can also be seen from Fig. 12 that each two adjacent ACFs has a small overlap, which is to prevent the unknown frequency at the edge of the ACF from being ignored due to errors. If the microwave frequency is measured at both overlapping parts, the measurement result in the low frequency band was chosen.

By using the calibrated multi-band mean ACFs shown in Fig. 12 and set the optical carrier wavelengths according to Table 1, we measured microwave frequencies in the range of 5∼40 GHz with 20 MHz frequency step for ten times. The relationship between the measured and actual input frequencies is shown in Fig. 13(a), and the corresponding measurement errors are shown in Fig. 13(b).The maximum measurement error is limited in ±180 MHz, and the maximum RMSE is

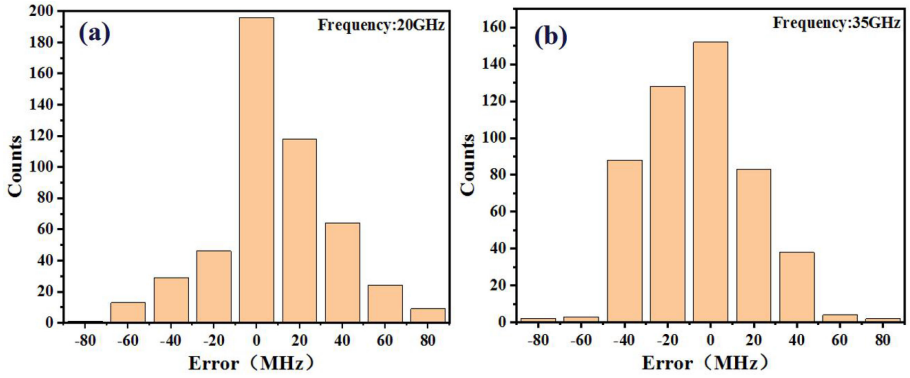

Fig. 14. The frequency measurement error distributions at (a) 20 GHz and (b) 35 GHz.

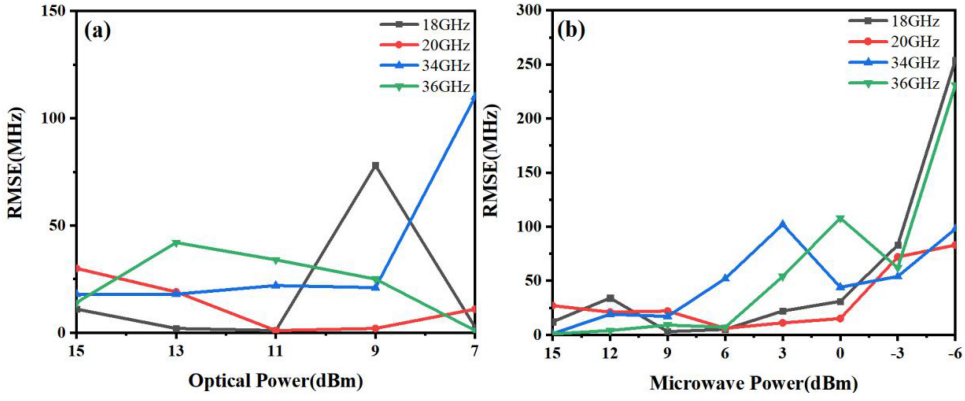

Fig. 15. Variation of RMSE with (a) optical power and (b) microwave power.

no more than 37 MHz. Obviously, the proposed multi-band measurement inherits the advantages of high accuracy of single-band measurement then the trade-off between the measurement range and accuracy is overcome.

In order to evaluate the frequency measurement accuracy of this system, we input two microwave signals with frequencies of 20 GHz and 35 GHz. After 500 measurements„ the errors were obtained as shown in Fig. 14. When the input frequency is 20 GHz, 72% of the errors are limited in ±20 MHz. When the input frequency is 35 GHz, the measurement error is larger, which may be due to the lower RF response of the measurement system at higher frequencies, but the overall error can still be well controlled within about ± 50 MHz.

In addition, we also investigated the influences of the powers of the optical carrier and microwave signals on the measurement accuracy. We selected four frequencies (18 GHz, 20 GHz, 34 GHz and 36 GHz) and the measurements were performed five times under different optical carrier powers or microwave powers. The obtained RMSEs are plotted in Fig. 15. From Fig. 15(a), it can been seen the RMSE generally increase as the optical carrier power decreases, and it does not change much when the optical power is larger than 9 dBm. Fig. 15(b) shows that as the microwave power decreases, the RMSE generally increases too, especially when the microwave power drops below 3 dBm. Considering that the power of the received microwave signal is not very high in practical applications, the received microwave signal can be amplified by a microwave power amplifier before being measured.

4. Conclusion

A microwave frequency measurement system based on a silicon nitride ring assisted Mach-Zehnder interferometer (RAMZI) is demonstrated. By using the microwave frequency to optical power mapping method, two ACFs were obtained by selecting two RAMZI configurations. A high-precision frequency measurement with root mean square error (RMSE) of less than 30 MHz was achieved in a frequency range of 5.2 GHz, and relative low-precision frequency measurement with a RMSE of less than 102 MHz was achieved in a frequency range of 11 GHz. Besides, a multi-band measurement method was proposed to break the trade-off between measurement range and measurement accuracy, and frequency measurement range of 5∼39 GHz with RMSE lower than 37 MHz was achieved. Finally, it should be pointed out that the jitter of the light source, the temperature change, and the manufacturing error of the chip will cause errors in the measurement results. Solving the influence of these factors is expected to further improve the measurement accuracy of the system. After this proof of concept experiment, we are now working on assembling the laser, RAMZI chip, photodetector, power supply and other components into a compact package, which could be used as a frequency module. In the future, by integrating the semiconductor laser, modulator and photodetector using the hybrid integration technology, even compact, low power and stable frequency measurement system can be achieved.

References

[1] T. A. Nguyen, E. H. Chan and R. A. Minasian, "Instantaneous high-resolution multiple-frequency measurement system based on frequency-to-time mapping technique," *Opt. Lett.*, vol. 39, no. 8, pp. 2419–2422, 2014.

[2] J. Capmany and D. Novak, "Microwave photonics combines two worlds," *Nature Photon.*, vol. 1, no. 6, pp. 319–330, 2007.

[3] A. J. Seeds and K. J. Williams, "Microwave photonics," *J. Lightw. Technol.*, vol. 24, no. 12, pp. 4628–4641, Dec. 2006.

[4] S. Pan and J. Yao, "Photonics-based broadband microwave measurement," *J. Lightw. Technol.*, vol. 35, no. 16, pp. 3498–3513, Aug. 2017.

[5] S. T. Winnall and A. C. Lindsay, "A Fabry-Perot scanning receiver for microwave signal processing," *IEEE Trans. Microw. Theory Techn.*, vol. 47, no. 7, pp. 1385–1390, Jul. 1999.

[6] G. Tengstrand, O. Tarasenko, C. Sterner, W. Margulis, P. Rugeland, and Z. Yu, "Photonic scanning receiver using an electrically tuned fiber Bragg grating," *Opt. Lett.*, vol. 34, no. 24, pp. 3794–3796, 2009.

[7] H. Guo, G. Xiao, N. Mrad, and J. Yao, "Measurement of microwave frequency using a monolithically integrated scannable echelle diffractive grating," *IEEE Photon. Technol. Lett.*, vol. 21, no. 1, pp. 45–47, 2009.

[8] S. Zheng, S. Ge, X. Zhang, H. Chi, and X. Jin, "High-resolution multiple microwave frequency measurement based on stimulated brillouin scattering," *IEEE Photon. Technol. Lett.*, vol. 24, no. 13, pp. 1115–1117, Jan. 2012.

[9] F. Zhou, H. Chen, X. Wang, L. Zhou, J. Dong, and X. Zhang, "Photonic multiple microwave frequency measurement based on frequency-to-time mapping," *IEEE Photon. J.*, vol. 10, no. 2, Apr. 2018, Art. no. 5500807.

[10] B. Vidal, T. Mengual, and J. Marti, "Photonic technique for the measurement of frequency and power of multiple microwave signals," *IEEE Trans. Microw. Theory Techn.*, vol. 58, no. 11, pp. 3103–3108, Nov. 2010.

[11] Y. Wang, X. Jin, S. Zheng, H. Chi, and X. Zhang, "Photonic approach for microwave spectral analysis based on Fourier cosine transform," *Opt. Lett.*, vol. 36, no. 19, pp. 3897–3899, 2011.

[12] R. Li, H. Chen, Y. Yu, M. Chen, S. Yang, and S. Xie, "Multiple-frequency measurement based on serial photonic channelization using optical wavelength scanning," *Opt. Lett.*, vol. 38, no. 22, pp. 4781–4784, 2013.

[13] J. M. Heaton *et al.*, "16-channel (1- to 16-GHz) microwave spectrum analyzer device based on a phased array of GaAs/AlGaAs electro-optic waveguide delay lines," in *Proc. Integr. Opt. Devices II*, 1998, pp. 245–251.

[14] R. Lodenkamper *et al.*, "Characterization of a coherent optical RF channelizer based on a diffraction grating," *IEEE Trans. Microw. Theory Techn.*, vol. 49, no. 10, pp. 1996–2001, Oct. 2001.

[15] D. B. Hunter, L. G. Edvell, and M. A. Englund, "Wideband microwave photonic channelised receiver," in *Proc. Microw. Photon. MWP. Int. Topical Meeting*, 2005, pp. 249–252.

[16] S. T. Winnall, A. C. Lindsay, M. W. Austin, J. Canning, and A. Mitchell, "A microwave channelizer and spectroscope based on an integrated optical bragg-grating Fabry-Perot and integrated hybrid fresnel lens system," *IEEE Trans. Microw. Theory Techn.*, vol. 54, no. 2, pp. 868–872, Feb. 2006.

[17] X. Zou, W. Pan, B. Luo, and L. Yan, "Photonic approach for multiple-frequency-component measurement using spectrally sliced incoherent source," *Opt. Lett.*, vol. 35, no. 3, pp. 438–440, 2010.

[18] X. Xie *et al.*, "Broadband photonic RF channelization based on coherent optical frequency combs and I/Q demodulators," *IEEE Photon. J.*, vol. 4, no. 4, pp. 1196.1202, Aug. 2012.

[19] X. Zou and J. Yao, "An optical approach to microwave frequency measurement with adjustable measurement range and resolution," *IEEE Photon. Technol. Lett.*, vol. 20, no. 23, pp. 1989–1991, Dec. 2008.

[20] X. Zhang, C. Hao, X. Zhang, S. Zheng, X. Jin, and J. Yao, "Instantaneous microwave frequency measurement using an optical phase modulator," *IEEE Microw. Wireless Components Lett.*, vol. 19, no. 6, pp. 422–424, Jun. 2009.

[21] Y. Li, L. Pei, J. Li, Y. Wang, and J. Yuan, "Theory study on a range-extended and resolution-improved microwave frequency measurement," *J. Modern Opt.*, vol. 63, no. 7, pp. 613–620, 2016.

[22] N. H. Zhu, L. X. Wang, and W. Li, "Brillouin-assisted microwave frequency measurement with adjustable measurement range and resolution," *Opt. Lett.*, vol. 37, no. 2, pp. 166–168, 2012.
[23] S. Pan and J. Yao, "Instantaneous microwave frequency measurement using a photonic microwave filter pair," *IEEE Photon. Technol. Lett.*, vol. 22, no. 19, pp. 1437–1439, Oct. 2010.
[24] D. Marpaung, "On-chip photonic-assisted instantaneous microwave frequency measurement system," *IEEE Photon. Technol. Lett.*, vol. 25, no. 9, pp. 837–840, May 2013.
[25] L. Liu, H. Qiu, Z. Chen, and Z. Yu, "Photonic measurement of microwave frequency with low-error based on an optomechanical microring resonator," *IEEE Photon. J.*, vol. 9, no. 6, Dec. 2017, Art. no. 5503611.
[26] L. Liu, W. Xue, and J. Yue, "Photonic approach for microwave frequency measurement using a silicon microring resonator," *IEEE Photon. Technol. Lett.*, vol. 31, no. 2, pp. 153–156, Jan. 2018.
[27] S. N., M. A., B. L., and E. H., "Reduced cost photonic instantaneous frequency measurement system," *IEEE Photon. Technol. Lett.*, vol. 20, no. 18, pp. 1521–1523, Sep. 2008.
[28] R. N. Nogueira, C. A. F. Marques, P. P. Monteiro, and M. V. Drummond, "Photonic instantaneous microwave frequency measurement system based on signal remodulation," *IEEE Photon. Technol. Lett.*, vol. 22, no. 16, pp. 1226–1228, Aug. 2010.
[29] L. A. Bui *et al.*, "Instantaneous frequency measurement system using optical mixing in highly nonlinear fiber," *Opt. Express*, vol. 17, no. 25, pp. 22983–22991, 2009.
[30] L. A. Bui, N. Sarkhosh, and A. Mitchell, "Photonic instantaneous frequency measurement: Parallel simultaneous implementations in a single highly nonlinear fiber," *IEEE Photon. J.*, vol. 3, no. 5, pp. 915.925, Oct. 2011.
[31] M. Pagani, K. Vu, D. Choi, S. J. Madden, B. J. Eggleton, and D. Marpaung, "Instantaneous microwave frequency measurement using four-wave mixing in a chalcogenide chip," *Opt. Commun.*, vol. 373, pp. 100–104, 2016.
[32] X. Zou, H. Chi, and J. Yao, "An approach to the measurement of microwave frequency based on optical power monitoring," *IEEE Photon. Technol. Lett.*, vol. 20, no. 14, pp. 1249–1251, Jul. 2008.
[33] J. Yao, X. Zou, and H. Chi, "Microwave frequency measurement based on optical power monitoring using a complementary optical filter pair," *IEEE Trans. Microw. Theory Techn.*, vol. 57, no. 2, pp. 505–511, Feb. 2009.
[34] X. Zou, W. Pan, B. Luo, and L. Yan, "Full-scale phase demodulation approach for photonic instantaneous frequency measurement," *Opt. Lett.*, vol. 35, no. 16, pp. 2747–2749, 2010.
[35] M. V. Drummond, P. Monteiro and R. N. Nogueira, "Photonic RF instantaneous frequency measurement system by means of a polarization-domain interferometer," *Opt. Express*, vol. 17, no. 7, pp. 5433–5438, 2009.
[36] J. S. Fandiño and P. Muñoz, "Photonics-based microwave frequency measurement using a double-sideband suppressed-carrier modulation and an InP integrated ring-assisted Mach-Zehnder interferometer filter," *Opt. Lett.*, vol. 38, no. 21, pp. 4316–4319, 2013.
[37] Y. Li, Z. Zhao, C. Li, C. Zhu, J. Zhang, and X. Yang, "Instantaneous microwave frequency measurement using an asymmetric integrated optical waveguide Mach-Zenhder interferometer (AMZI)," *Optik*, vol. 169, pp. 203–207, 2018.
[38] J. Jiang *et al.*, "Photonic-assisted microwave frequency measurement system based on a silicon ORR," *Opt. Commun.*, vol. 382, pp. 366–370, 2017.
[39] H. Yang, J. Li, P. Zheng, G. Hu, B. Yun, and Y. Cui, "A stopband and passband switchable microwave photonic filter based on integrated dual ring coupled Mach–Zehnder interferometer," *IEEE Photon. J.*, vol. 11, no. 4, Aug. 2019, Art. no. 5502608.
[40] W. Hoving, R. Heideman, D. Geuzebroek, A. Leinse, E. Klein, and R. Dekker, "Low loss, high contrast planar optical waveguides based on low-cost CMOS compatible LPCVD processing," in *Proc. SPIE*, 2008, Art. no. 699612.